Tapping Mode Atomic Force Microscopy Investigation of Poly(amidoamine) Dendrimers: Effects of Substrate and pH on Dendrimer Deformation

Theodore A. Betley, Mark M. Banaszak Holl,* Bradford G. Orr,* Douglas R. Swanson, Donald A. Tomalia, and James R. Baker, Jr.

Departments of Chemistry and Physics and the Center for Biologic Nanotechnology, University of Michigan, Ann Arbor, Michigan 48109-1055

Received September 11, 2000. In Final Form: February 9, 2001

Substrate effects, volume reproducibility, and pH effects on the size and shape of ethylenediamine core poly(amidoamine) dendrimers (generations 6−9) were explored using tapping mode atomic force microscopy (AFM) measurements. A statistical analysis of the measurements indicated a 4% variation in volume for repeated measurement using the same tip. Volume determinations by numerical integration and a spherical cap estimation method were explored. The spherical cap model was shown to overestimate dendrimer volumes by a factor of ∼2. As substrates were changed from mica to more hydrophobic surfaces, AFM-measured heights and diameters approached ideal-sphere dendrimer diameters. Acidification of dendrimer samples from generations 6−9 led to an observed 33% increase in volume, 26% increase in height, and 9% decrease in diameter. Expansion upon acidification can be attributed to maximization of charge separation and increased solvent retention within the dendrimers. Single dendrimer resolution within two-dimensional clusters was enhanced using carbon nanoprobes.

Introduction

Dendrimeric polymers can be readily synthesized in appropriate size ranges and with the needed surface functionality to readily interact with biologically important entities such as DNA and cells.[1−8] These properties have led to consideration of dendrimeric polymers, specifically polyamidoamine (PAMAM) starburst dendrimers, as promising drug transport agents (Figure 1). Initial reports describing the use of PAMAM dendrimers to transport DNA into cells are quite promising.[4,5] To function as a transport agent, the PAMAM dendrimer must pass through and interact with a number of complex biological interfaces including the cell and nuclear membranes. To better understand the structural properties of these polymers and their behavior at interfaces, we have initiated a series of atomic force microscopy (AFM) studies to explore the surface interaction of PAMAM dendrimers.

Previous workers noted that surface-adsorbed PAMAM dendrimers are significantly distorted from the ideal spherical dendrimer geometry.[9−13] This type of behavior has also been observed for other classes of dendrimers.[14] Crooks et al. found the interpretation of the images to be complicated by uncertain amounts of tip convolution in the lateral dimensions.[9] This makes volume determinations uncertain. Both they and Tsukruk et al. noted that dendrimers interacted much more strongly, as indicated by the degree of structural distortion, with the surface in the absence of neighboring dendrimers or other organic molecules such as alkanethiols. More recently, Li et al. were able to estimate dendrimer volumes using a spherical-cap approximation that appeared to be in reasonable accord with expectations based upon theoretical and experimental criteria.[11]

Upon the basis of these previous studies, we implemented the experiments described in this report with the following questions in mind: (1) How elastic is the PAMAM dendrimer structure with respect to surface interaction? (2) Can one make volume measurements using AFM with sufficient accuracy and reproducibility to detect dendrimer aggregation and/or dendrimer defects? In addition, inspired by the concerns of Crooks et al. that tip convolution was playing a significant role in the lateral dimensions measured,[9,10] we were interested in measuring the particle diameters using a carbon nanoprobe tip of the type described by Lieber et al.[15−18]

Experimental Section

The goal of this study was to use AFM to image dendrimers under varying conditions and determine the systematic changes

(1) Tomalia, D. A. *Sci. Am.* **1995**, *272*, 42−46.
(2) Chen, W.; Turro, N. J.; Tomalia, D. A. *Langmuir* **2000**, *16*, 15−19.
(3) Ottaviani, M. F.; Sacchi, B.; Turro, N. J.; Chen, W.; Jockusch, S.; Tomalia, D. A. *Macromolecules* **1999**, *32*, 2275−2282.
(4) Bielinska, A.; Kukowska-Latallo, J. F.; Johnson, J.; Tomalia, D. A.; Baker, J. R. *Nucleic Acids Res.* **1996**, *24*, 2176−2182.
(5) Kukowska-Latallo, J. F.; Bielinska, A. U.; Johnson, J.; Spindler, R.; Tomalia, D. A.; Baker, J. R. *Proc. Natl. Acad. Sci. U.S.A.* **1996**, *93*, 4897−4902.
(6) Zeng, F.; Zimmerman, S. C. *Chem. Rev.* **1997**, *97*, 1681−1712.
(7) Singh, P. *Bioconjugate Chem.* **1998**, *9*, 54−63.
(8) Bosman, A. W.; Janssen, H. M.; Meijer, E. W. *Chem. Rev.* **1999**, *99*, 1665−1688.
(9) Hierlemann, A.; Campbell, J. K.; Baker, L. A.; Crooks, R. M.; Ricco, A. J. *J. Am. Chem. Soc.* **1998**, *120*, 5323−5324.
(10) Tokuhisa, H.; Zhao, M.; Baker, L. A.; Phan, V. T.; Dermody, D. L.; Garcia, M. E.; Peez, R. F.; Crooks, R. M.; Mayer, T. M. *J. Am. Chem. Soc.* **1998**, *120*, 4492−4501.
(11) Li, J.; Peihler, L. T.; Qin, D.; Baker, J. R.; Tomalia, D.; Meier, D. *Langmuir* **2000**, *16*, 5613−5616.
(12) Tsukruk, V. V.; Rinderspacher, R.; Bliznyuk, V. N. *Langmuir* **1997**, *13*, 2171−2176.
(13) Bliznyuk, V. N.; Rinderspacher, F.; Tsukruk, V. V. *Polymer* **1998**, *39*, 5249−5252.
(14) Takada, K.; Díaz, D.; Abruña, H. D.; Cuadrado, I.; Casado, C.; Alonso, B.; Morán, M.; Losada, J. *J. Am. Chem. Soc.* **1997**, *119*, 10763−10773.
(15) Wong, S. S.; Harper, J. D.; Lansbury, P. T.; Lieber, C. M. *J. Am. Chem. Soc.* **1998**, *120*, 603−604.
(16) Cheung, C. L.; Hafner, J. H.; Odom, T. W.; Kim, K.; Lieber, C. M. *Appl. Phys. Lett.* **2000**, *76*, 3136−3138.
(17) Hafner, J. H.; Cheung, C. L.; Lieber, C. M. *Nature* **1999**, *398*, 761−762.
(18) Hafner, J. H.; Cheung, C. L.; Lieber, C. M. *J. Am. Chem. Soc.* **1999**, *121*, 9750−9751.

10.1021/la001297h CCC: $20.00
Published on Web 04/05/2001

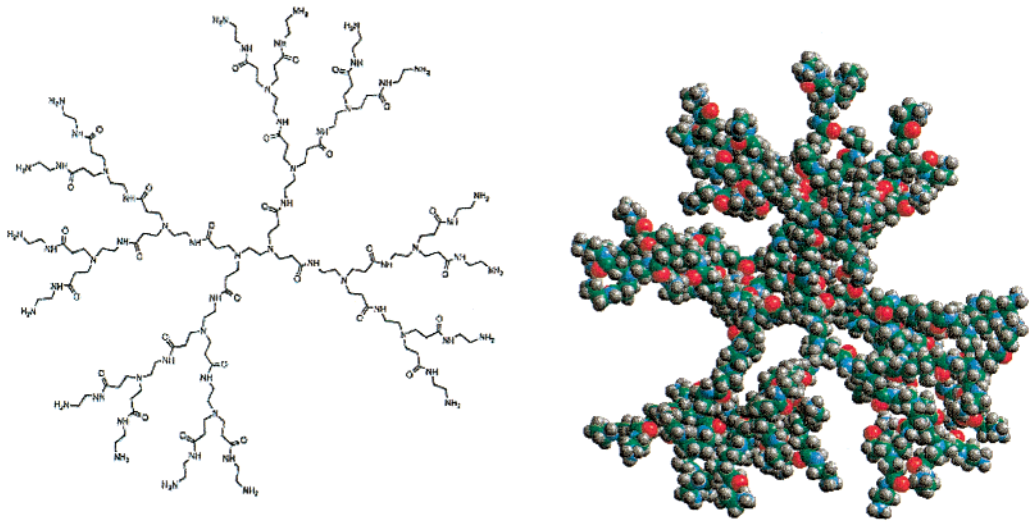

A **B**

Figure 1. (A) Schematic chemical structure of a generation 3 (G3) PAMAM dendrimer based upon an ethylenediamine core. Each generation is grown by the sequential addition of vinyl acetate and ethylenediamine. The number of surface primary amines doubles with each generation. Theoretically, the G9 dendrimers studied in this work contain 2048 surface primary amines. (B) A space-filling model of a G4 PAMAM dendrimer in an isotropic environment.

induced by the environment in the images. The sample material used for the study was ethylenediamine (EDA) core poly(amidoamine) dendrimers (generations 6−9). The samples were obtained as methanol solutions from the University of Michigan's Center for Biologic Nanotechnology. The solutions were typically diluted to 1 nM concentrations with deionized, distilled, Millipore (0.1 μm) filtered water and stored at −4 °C until use.

Substrate Preparation. Three different substrates were used during the course of this study. Mica substrates were prepared by cleaving to produce a clean, smooth surface prior to sample deposition. Trimethylsilane-terminated silicon substrates (SiO_2-TMS) were prepared by rinsing Si(111) wafers with ethanol and then soaking the silicon in chlorotrimethylsilane for 20 min. The TMS-terminated silica surface was then dried under flowing air prior to sample deposition. Hydridosilsesquioxane (HSQ) resin (also known as FOx resin) was obtained from Dow Corning and used without further purification. A thin film was produced by spin-coating the HSQ resin dissolved in methylisobutyl ketone (60 mg/cc) at 1300 rpm onto a freshly cleaved mica surface.

Sample Preparation. Sample solutions of dendrimers (typically 1−5 nM in concentration with a pH of either ∼7 or ∼1) were spin-coated on substrates at 100−200 rpm in air for 5 min. Aqueous dendrimer solutions were acidified to pH ∼ 1 by dropwise addition of concentrated hydrochloric acid (12.6 M). The sample pH was verified using litmus paper.

AFM Measurements. All measurements were made using tapping mode operation with a Nanoscope IIIa Multimode scanning probe microscope from Digital Instruments (Santa Barbara, CA) using a "J" vertical engage scanner. Tapping mode etched silicon probes (TESP; manufacturer specifications: spring constant $k_0 = 40-71$N/m, force constant $f_0 = 351-422$ kHz) and carbon nanoprobes were used for imaging. The carbon nanoprobes were grown on force etched silicon probes (FESP; manufacturer specifications: $k_0 = 1.7-2.9$ N/m, $f_0 = 70-83$ kHz) using literature procedures.[16−18] The radii of curvature for both commercial TESP and carbon nanoprobes were measured using Nioprobe standards available from GeneralMicro.[19,20] The carbon nanoprobe tips used for this study were measured prior to obtaining dendrimer images and had a radius of curvature of 2.6 ± 0.2 nm consistent with the literature.[18] Representative TESP tips were measured and determined to have radii of 3.9 and 4.2 nm, consistent with manufacturer specifications. Tip convolution was determined by subtracting the tip geometry contribution from cross-sectional line scans. For the purposes of the calculations, tip geometry was assumed to be spherical with diameters as reported in the literature (carbon nanoprobes, $d_{tip} = 2.5$ nm; TESP probes, $d_{tip} = 4$ nm from manufacturer specifications).[18] The purpose for determining the tip convolution was to estimate volume increases to AFM images as a function of aspect ratios. As described in the results section, essentially identical results were obtained for the G9 dendrimers from both kinds of tips. Error in the reproducibility of the measurements exceeded any measurable differences in tip convolution for these low aspect ratio samples.

Calculations. Densities of PAMAM dendrimers have been reported for generations 0−5.[21] To estimate the densities of later generations, the published densities were fit to a saturation model in the form of

$$\text{density (g/cm}^3) = a - be^{(-cn)}$$

where a, b, and c are empirical parameters and n is the generation number. The values for the parameters are $a = 1.232$, $b = 0.05540$, and $c = 0.4741$.

The volumes for the samples in the AFM images were determined via numerical integration of the data using the bearing calculations included in the instrumental software. The largest pixel size used for determining sample volume was 3 × 3 Å.

Results and Discussion

This study is centered on AFM imaging of PAMAM dendrimers utilizing various environmental conditions. Reproducibility of the AFM images will be discussed first. Experimental reproducibility determines the precision that can reasonably be attributed to the variety of measurements reported. The effects of three factors, substrate, pH, and tip radius, upon the image obtained will be discussed.

Experimental Reproducibility. AFM is useful for visualizing the uniformity of dendrimer samples; however, a detailed statistical analysis on the reproducibility of the height and diameter measurements for dendrimer samples

(19) Westra, K. L.; Thomson, D. J. *J. Vac. Sci. Technol., B* **1994**, *12*, 3176−3181.

(20) Westra, K. L.; Mitchell, A. W.; Thomson, D. J. *J. Appl. Phys.* **1993**, *74*, 3608−3610.

(21) Uppuluri, S.; Keinath, S. E.; Tomalia, D. A.; Dvornic, P. R. *Macromolecules* **1998**, *31*, 4498−4510.

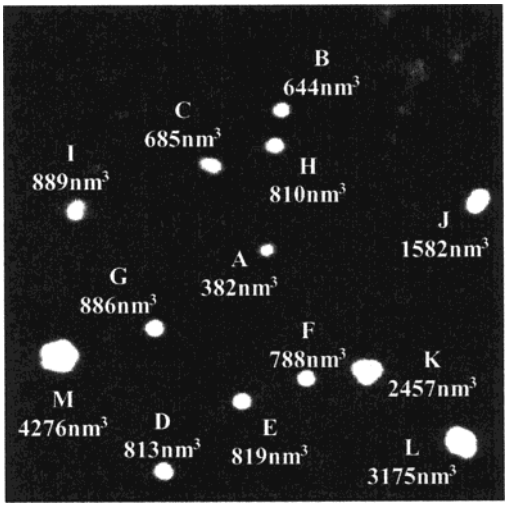

Figure 2. AFM image obtained by spin-coating a pH = 1 aqueous solution of G9 PAMAM dendrimers onto a mica substrate (500 × 500 nm, vertical scale = 5 nm). The dendrimers and dendrimer clusters are labeled with their measured volumes.

has not been reported. Claims about sample quality can be made if the uncertainty in the measurement precision is significantly less than the structural variation between individual polymer particles.

To determine the statistical variation in AFM measurements, a sample of ninth generation (G9) PAMAM dendrimers was imaged repeatedly to quantify the variation between consecutive scans, piezo shifts, and scan size changes (Figure 2). The solution from which the sample was deposited was acidified with hydrochloric acid to a pH of 1 to reduce particle aggregation during deposition. After stable imaging conditions were reached (no streaking apparent during imaging and the trace and retrace images were consistent), the uncertainty or variation between consecutive measurements was 4%, where the uncertainty is the standard deviation divided by the mean measurement per particle. Table 1 lists the volumes of the nine particles shown in Figure 2 compiled over a series of five measurements that are representative of the observed data. The reproducibility of the AFM measurements shows that the volume difference between the individual particles is not an artifact of the measurement itself.

Volume Statistics. The overarching motivation of this study was the determination of the uniformity of dendrimer volume. To obtain a better understanding of these issues, exploration of the parameters that could affect the interpretation and analysis of the AFM images was necessary. For these images, samples were acidified to pH = 1 to minimize dendrimer aggregation. Choice of deposition pH does dramatically affect absolute sample volume but does not change the observed distribution of volumes.

The theoretical volume of neutral G9 dendrimers is 630 nm^3 (based upon ideal molecular weight and an estimated sample density of 1.232 g/cm^3). The largest generation PAMAM dendrimer with an experimentally measured density is G5 (1.220 g/cm^3).[21] The experimental hydrodynamic radius of 5.7 nm measured by light scattering yields a volume of 776 nm^3.[11] The estimated volume of a G9 dendrimer with all the internal and primary amines protonated and a single water molecule associated with each amine is 840 nm^3, assuming a sphere of constant density. These three approaches yield a range of estimates for the G9 dendrimer volumes measured by AFM.

The particle volumes in Figure 2 range from 380 to 4300 nm^3. Elements D−M show good overall consistency for the individual dendrimer volumes. The standard deviation (5% of the average G9 volume) of the volume measurements for particles D−I is the same order of magnitude as the variation (4%) expected in consecutive scans on the same molecule. Thus, within the uncertainty of the measurements, the dendrimers labeled D−I and the individual dendrimers making up particles J−M have identical volumes. The average volume for the acidified individual G9 dendrimers (D−I) was 834 ± 42 nm^3. A carbon nanoprobe tip was also used to study the same sample. The average volume measured in this case was 804 ± 19 nm^3. Although it might be tempting to ascribe this decrease in volume to differences in tip convolution, it must be noted that this difference in measured volumes is just 4% and thus within the range of the experimental error for multiple measurements on the same sample.

Particles consisting of clusters of two, three, four, and five dendrimers (labeled J, K, L, and M, respectively) are readily apparent in the topography image (Figure 2). The total volumes of these clusters correlate with integer multiples of 820 ± 29 nm^3. This is in good agreement with the average volume measured for the individual dendrimers. The dendrimers labeled A−C in Figure 2 have volumes sufficiently different from the average to be unaccounted for by the measurement uncertainty.

Possible mechanisms for the discrepancies between individual dendrimers in Figure 2 include tip convolution, varying degrees of amine protonation and solvent retention, or structural differences in the polymers themselves (e.g., missing branches). Theoretical modeling of tip convolution effects indicated that the volumes measured in this work for 2.5 nm tips are increased no more than 3−10% (the variance is due to the dendrimer asymmetry). AFM measurements on the same G9 sample using multiple TESP, FESP, and carbon nanoprobe tips yielded comparable variation in height and diameter data to that illustrated in Figure 2. The individual tip convolutions did not affect the reproducibility or the magnitude of the computed volumes. Over the range of aspect ratios represented in Figure 2, no tip effects could be ascertained.

The pH of the dendrimer sample prior to deposition was sufficient to protonate all the internal dendrimer amines,[22] and thus incomplete protonation is not expected to be an issue. However, the volumes of B and C are remarkably similar to that predicted (and measured) for neutral dendrimers. Therefore, neutralization of these particles cannot be definitively ruled out. Solvent retention cannot be quantified per molecule without complementary analytical techniques, but the volume magnitudes did not change considerably after the same sample was heated to 40 °C for 1 h to remove excess solvent. Solvent has been shown to effect the radius of gyration of dendrimers by ∼10%.[23]

The observed discrepancies between the individual particles may arise from differences in the polymers themselves. Dendrimer A in Figure 2 most likely has imperfections that cause a deviation from the average observed volume. This is likely the case for dendrimers B and C as well. Using molecular weights derived from the volumes observed, the polydispersity of the sample (based on 25 molecular volumes) is calculated to be 1.2 (M_W/M_N). Previous measurements for G9 dendrimers on mica found a somewhat lower polydispersity (1.08).[11]

(22) van Duijvenbode, R. C.; Borkovec, M.; Koper, G. J. M. *Polymer* **1998**, *39*, 2657−2664.
(23) Topp, A.; Bauer, B. J.; Tomalia, D. A.; Amis, E. J. *Macromolecules* **1999**, *32*, 7232−7237.

Table 1. Sample Statistical Data on Volume Reproducibility Experiment

measurement	V_A (nm^3)	V_B (nm^3)	V_C (nm^3)	V_D (nm^3)	V_E (nm^3)	V_F (nm^3)	V_G (nm^3)	V_H (nm^3)	V_I (nm^3)
1	367	672	690	798	804	792	865	762	890
2	396	643	686	829	835	823	914	805	896
3	374	594	661	817	830	791	873	799	874
4	405	645	705	844	867	805	899	847	918
5	366	666	681	779	757	731	880	837	865
$V_{average}$	**382**	**644**	**685**	**813**	**819**	**788**	**886**	**810**	**889**
$V_{stdeviation}$	18	31	16	26	41	35	20	34	21
$V_{uncertainty}$	4.7%	4.8%	4.8%	3.1%	5.0%	4.4%	2.3%	4.2%	2.3%
average									**3.7%**

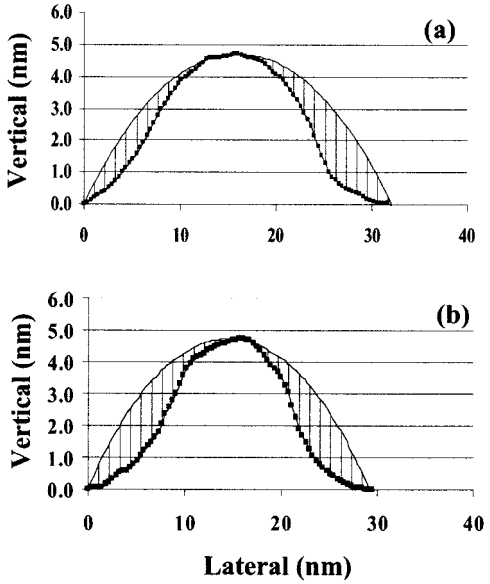

Figure 3. Horizontal (a) and vertical (b) line scans measured for dendrimer E (Figure 2). The inner line is the experimentally measured topography, and the outer line represents the topography of a spherical cap of the same height. The shaded region is the excess area (in two dimensions) that becomes excess volume when the surfaces are convolved into three dimensions.

The volumes of the individual molecules and clusters were determined via numerical integration of the data (i.e., the bearing method). Numerically integrated volumes are more accurate than volumes determined using a spherical-cap approximation. Because of the asymmetries in the individual molecules and nonconstant concavity of the samples, the spherical cap typically overestimates the particle volume by a factor of ~2. Figure 3 shows the horizontal (a) and vertical (b) line scans for dendrimer E of Figure 2. The corresponding cross section of the spherical cap used to estimate the molecular volume is shown as the outer line for both cases. The shaded area between the experimental line scan and the spherical-cap cross section becomes excess volume when convolved into three dimensions. The volume yielded by the spherical-cap model from line scan (a) is 1950 nm^3, 225% of the volume determined by numerical integration of 867 nm^3. The volume yielded by the spherical-cap model for line scan (b) is 1630 nm^3 (188% of the integrated volume). Both horizontal and vertical line scans are provided to highlight the asymmetries in individual particles. Note that the two line scans give spherical-cap volume estimates which differ by ~20%, far greater than the average experimental reproducibility (~4%) that we measured using the data in Figure 2 and numerical integration methods. Numerical integration of sample volume is unaffected by the molecule asymmetry and will yield accurate volume calculations.

Substrate Effect. It is known from previous work that the substrate plays a large role in the imaging of dendrimer samples. Researchers have observed that significant flattening of dendrimers occurs with substrate surfaces of mica, gold, and platinum.[9−11,14] Deviations as much as 60% from the theoretical dendrimer diameters have been reported.[9] A general model for dendrimer deformation with surfaces has been proposed.[24] For PAMAM dendrimers, it is proposed that interactions between the dendrimer primary amine cap and the substrate cause this distortion of the particle. If this is true, as the substrate surface becomes increasingly hydrophobic and interactions between the sample and substrate decrease to weaker hydrogen bonds and van der Waals forces, distortion of the dendrimer should decrease. Where sample−substrate interaction is minimal, the apparent height of the dendrimer samples will be larger and a concomitant decrease in the observed diameter is expected.

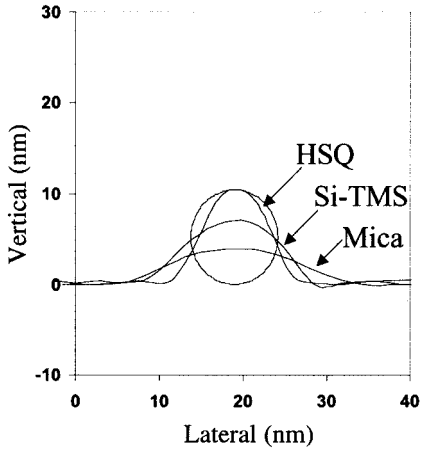

Figure 4. A comparison of the line scans for individual G9 dendrimers deposited from pH = 1 aqueous solutions onto mica, SiO_2-TMS, and HSQ resin. The ideal spherical diameter is indicated by a circle. The volumes measured for the dendrimers are 790 nm^3 (mica), 870 nm^3 (SiO_2-TMS), and 1190 nm^3 (HSQ).

Figure 4 illustrates this substrate effect on G9 dendrimers. Line scans for G9 on mica, SiO_2-TMS, and HSQ resin substrates show an increase from 4.5 nm on mica to 6.8 nm on SiO_2-TMS to 10.5 nm on HSQ resin. The single dendrimers used for the line scans have volumes of 794 nm^3 (mica), 869 nm^3 (SiO_2-TMS), and 1190 nm^3 (HSQ).

The change in volume is readily ascribed to a physical tip convolution artifact as the aspect ratio of the feature becomes greater. Assuming a tip diameter of 2.5 nm, we calculate an increase in apparent G9 volume of 14% (SiO_2-TMS) and 39% (HSQ) because of tip convolution. These are in reasonable agreement with the experimentally measured volume changes of 9% and 50%, respectively.

An additional effect of moving to a less interactive substrate is the degree to which dendrimers form aggregates as opposed to singly binding to the substrate. On both SiO_2-TMS and HSQ, the dendrimers tended to form

(24) Mansfield, M. L. *Polymer* **1996**, *37*, 3835−3841.

pillarlike aggregates. These pillars, with diameters of ~45−60 nm and heights of 15−20 nm, were estimated to contain as many as 25 individual dendrimers. For hydrophobic surfaces, finding large areas covered mainly by single dendrimers is very difficult and aggregates are the most commonly observed feature. Crooks et al. reported a similar effect. The adsorption of alkanethiols to gold surfaces induces aggregation of dendrimers into pillarlike structures.[9,10]

Utilizing more hydrophobic, less interactive substrates increases the aspect ratio of the dendrimers. As the aspect ratio of the sample increases, tip convolution becomes an important imaging artifact when considering the diameter or volume measurements; however, the height information should remain reliable. The G9 dendrimer height (10.5 nm) on HSQ approaches the ideal-sphere diameter (10.7 nm) and the diameter measured using light scattering experiments (11.4 nm).[11,25]

Sample pH Effect. When the primary and internal amines of a PAMAM dendrimer are protonated, the dendrimer should assume a more rigid structure to maximize charge separation within the molecule and be more prone to solvent coordination on charged centers. Aqueous solutions of PAMAM dendrimers from generations 6−9 were acidified to pH = 1 using concentrated 12.6 M hydrochloric acid and spin-coated onto mica substrates to see if an increase in molecular volume due to protonation and additional solvation was observable by AFM.

Figure 5 gives plots showing the volume, height, and diameter of generation 6−9 PAMAM dendrimers deposited from pH = 1 and pH = 6 solutions. The data compiled per generation are compared to the theoretical volumes based on known molecular weights and estimated densities per generation (extrapolation of densities from PAMAM dendrimer generations G0−G5).[21] The dendrimer samples for each generation come from the same stock solution diluted to a 0.5−1 nM concentration. One sample was subsequently acidified. The heights and diameters were measured using line scans over individual molecules, and the volume was determined by numerical integration. The data, summarized in Table 2, are a compilation of 15 particles per sample at each pH. Each particle measurement is averaged over a series of 3−5 scans.

The samples deposited from neutral solutions are close to the theoretical volumes (the mean observed volume is on average 120% of the theoretical value). The slightly larger than expected volume is likely caused by partial protonation of the primary amine surface, leading to volume expansion of the dendrimer. After acidification to pH = 1, the average volume increase for PAMAM dendrimers generations 6−9 was 33% ($V_{pH=1}/V_{pH=6}$). The height increase for the dendrimers was 26% ($h_{pH=1}/h_{pH=6}$), and the molecular diameter decreased by 9% (($d_{pH=1}/d_{pH=6}$)$_{AVG}$ = 91%). Vertical and horizontal line scans were averaged per molecule to determine the diameter. The increase in volume can be attributed to dendrimer expansion to maximize charge separation as well as an increase in solvent retention. Protonation of the amine groups will likely increase the amount of hydrogen bonding to the solvent molecules.

Enhanced Resolution Using Carbon Nanoprobes. Carbon nanoprobes were utilized in an attempt to increase lateral resolution on the dendrimer samples and, as previously discussed, to explore the role of tip convolution in the measurements. Measurements on single dendrimers did not reveal any new topographical information, suggesting that tip convolution on the lateral measurements was not a significant problem. However, imaging two-dimensional arrays of dendrimers did reveal some inter-dendrimer probing when using the carbon nanoprobe tips.

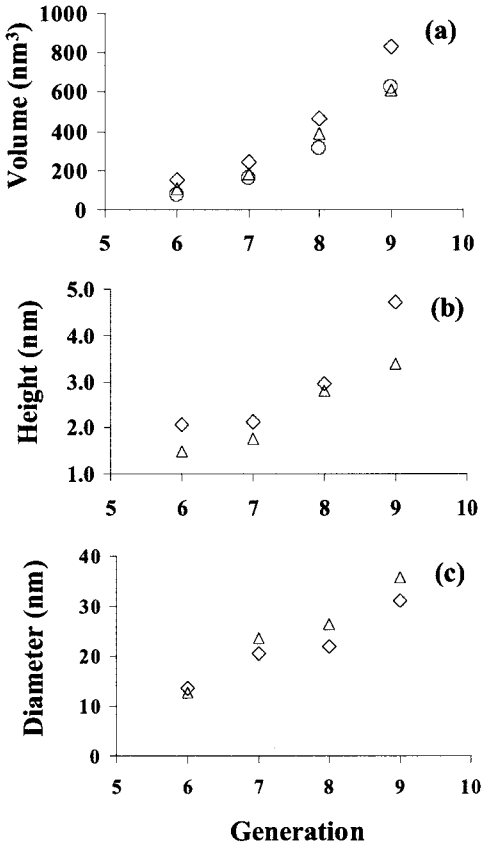

Figure 5. Changes in measured dendrimer dimensions upon deposition from solutions of pH = 1 (diamonds) and pH = 6 (triangles). The circles in panel a depict the theoretical volumes for generations 6−9 based on known molecular weights and estimated densities.

Figure 6 illustrates the enhanced lateral resolution obtained for a sample of G9 dendrimers spin-coated on mica. In panel a, a G9 image obtained with a TESP tapping mode tip is shown. Panel b shows the image for a similar dendrimer cluster obtained with a carbon nanoprobe tip. Line scan representations of a cluster containing four dendrimers imaged with a TESP tip (circle, panel a) and carbon nanoprobe tip (circle, panel b) highlight the increase in topographical information yielded by the carbon nanoprobe. Two dendrimer peaks are resolved when a carbon nanoprobe is scanned across the cluster. A maximum in the center of the cluster is an artifact of tip convolution when using the TESP tips. When imaged with a small diameter carbon nanoprobe tip, the presence of a minimum between the individual dendrimers is resolved. The highlighted tetramer cluster volumes determined by numerical integration are 3175 nm^3 (TESP) and 3300 nm^3 (carbon nanoprobe). The apparent discrepancy between line scan area and cluster volume is caused by individual cluster variation.

Panel d illustrates a line scan across a cluster containing seven dendrimers (cluster in panel b). Note the protrusion of the central dendrimer in the cluster. Favorable interactions, probably hydrogen bonding, with the surrounding dendrimers in the cluster appear to replace some of the interaction of the central dendrimer with the mica substrate. Thus, the dendrimer does not flatten as

(25) Dvornic, P. R.; Tomalia, D. A. *Poly(amidoamine) dendrimers*; Oxford University Press: Oxford, 1999.

Table 2. Dendrimer Dimensions[a]

	pH = 6				pH = 1			Δ		
	d (nm)	*h* (nm)	*V* (nm^3)	V_{THRY} (nm^3)	*d* (nm)	*h* (nm)	*V* (nm^3)	*d* (nm)	*h* (nm)	*V* (nm^3)
G6	13	1.5	110	78	14	2.1	155	1	0.6	45
G7	24	1.8	187	157	21	2.1	247	−3	0.4	60
G8	26	2.8	387	315	22	2.9	465	−4	0.1	77
G9	36	3.4	609	630	31	4.7	834	−5	1.3	225

[a] $\Delta = X_{pH=1} - X_{pH=6}$ where X = diameter (*d*), height (*h*), and volume (*V*).

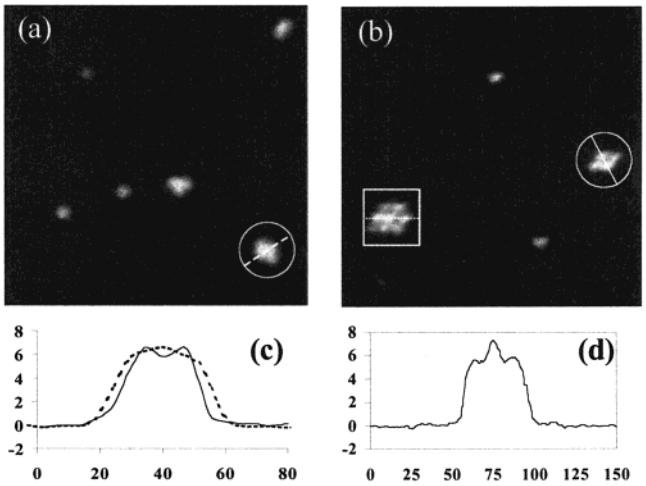

Figure 6. AFM images (300 × 300 nm) obtained by spin-coating a pH = 1 aqueous solution of G9 dendrimers onto a mica substrate. The images in panel a were obtained using a TESP tapping mode tip. The images in panel b were obtained using a carbon nanoprobe tip. Panel c compares the line scan images obtained for the TESP and carbon nanoprobe tips when measuring two different tetramers of dendrimers. Panel d shows the line scan for a carbon nanoprobe image of a dendrimer heptamer.

dramatically onto the mica substrate and a larger height is observed. Similar height effects were previously observed for adsorbing thiols to a dendrimer-coated gold substrate.[9]

Conclusions

The AFM experiments performed show the dramatic effects of substrate and pH of deposition solution upon the height, diameter, and volume of soft, deformable PAMAM dendrimers. On a sufficiently hydrophobic surface such as HSQ resin, the PAMAM dendrimers are no longer imaged as flat disklike structures. Rather, they exhibit the height anticipated based on theoretical and experimental prediction of the dendrimer diameter. These effects are highlighted in Figure 4. Both single dendrimers and clusters of dendrimers were directly imaged. Discrete dendrimer dimers, trimers, tetramers, pentamers, and heptamers were distinctly imaged and routinely shown to have volumes consistent with the addition of the appropriate integer number of dendrimers. The reproducibility of the volume measurements, ∼4%, is sufficiently good for AFM to serve as a useful probe of dendrimer sample quality.

Acknowledgment. This project has been funded in whole or in part with federal funds from the National Cancer Institute, National Institutes of Health, under Contract #NOI-CO-97111. M.M.B.H. thanks the Alfred P. Sloan Foundation for a Research Fellowship (1999-2002). H. Hansma and J. Li are thanked for fruitful discussions of this work. C. M. Lieber and his laboratory are thanked for providing a critical hands-on introduction to carbon nanoprobe techniques.

LA001297H